

Study of structural, optical and antibacterial properties of starch-capped Cu doped ZnO nanoparticles (NPs)

M. K. Debanath^{1*}, R. K. Saha¹, S. M. Borah¹, E. Saikia¹ and K. K. Saikia²

¹Department of Applied Sciences, Gauhati University, Guwahati, 781014, India

²Department of Bioengineering and Technology, Gauhati University, Guwahati, 781014, India

DOI: 10.5185/amp.2018/721

www.vbripress.com/amp

Abstract

In our present investigation, we have synthesized starch-capped Cu doped ZnO (ZnO:Cu) nanoparticles (NPs) by simple wet chemical method and studied their structural, optical and antibacterial effects on/against Gram-positive and Gram-negative bacteria. Chemically synthesized nanoparticle have been characterized using X-ray diffraction (XRD), scanning electron microscopy (SEM) with energy dispersive analysis of X-rays (EDAX), high resolution transmission electron microscopy (HRTEM), UV-vis absorption spectroscopy and photoluminescence (PL) spectroscopy for their structural and optical properties. Antibacterial properties have been studied by *Staphylococcus aureus* (*S. aureus*, Gram-positive) and *Escherichia coli* (*E. coli*, Gram-negative) bacteria. XRD study showed hexagonal wurtzite crystal structure of the prepared ZnO:Cu and nanoformation of the as-synthesized NPs. Nanoparticle formation have been finally confirmed by HRTEM analysis. Antibacterial studies showed excellent resistance of ZnO:Cu to *S. aureus* and *E. coli* respectively. Copyright © 2018 VBRI Press.

Keywords: ZnO:Cu nanoparticles; SEM; HRTEM; optical properties; antibacterial activity.

Introduction

Nanoparticles (NPs) have unique properties in physical appearance of the matter and chemical interactions due to its small sizes (< 100 nm) rather than their bulk equivalents. They show high antimicrobial properties, especially the ZnO due to their high surface to volume ratio. ZnO is an important II-VI wide-band-gap (3.3 eV, at 300K) semiconductor material which exhibits interesting properties including high exciton binding energy of 60 meV, strong adsorption ability and low growth temperature, providing for a wide variety of interesting applications [1, 2]. Recent studies have shown that ZnO nanoparticles have toxicity to bacterial cells but minimum effect on human cells. ZnO and CuO nanoparticles are used in industries for smart modifications to plastics, cosmetics etc [3]. The doped and undoped ZnO nanoparticles have been studied for antimicrobial activity with human pathogenic bacteria, mainly *Escherichia coli* (*E. coli*) and *Staphylococcus aureus* (*S. aureus*). Nano-ZnO are effective for inhibiting gram-positive and gram-negative bacteria, they show high activity against spores [4-8]. Smaller ZnO NPs (<< 100 nm) shows better antibacterial activity. The activity depends on the concentrations and surface area of the particles. The higher the concentration and larger the surface area, the better is the activity [4, 5, 9].

Synthesis and processing of nanostructures with high precision is significant to the advancement of nanoscience and nanotechnology. It is well known that properties and applications of nanostructure materials are possible only when they are made with desired size, morphology, and chemical composition. In addition, starch can be used as a capping agent that controls the particle size as well as stabilizing agent [10]. The present study focuses on the synthesis of starch-capped Cu doped ZnO NSs and its structural, optical and antibacterial activities of Cu doped ZnO NPs of as-prepared sample have been studied against *Staphylococcus aureus* (*S. aureus*, Gram-positive bacteria) and *Escherichia coli* [*E. coli*, Gram-negative bacteria, ATCC 25922 (antibiotic susceptible)] using well-diffusion method.

Experimental

Materials

All materials were purchased from the commercial market and used without further purification. Zinc nitrate hexahydrate [$Zn(NO_3)_2 \cdot 6H_2O$], copper chloride dehydrate ($CuCl_2 \cdot 2H_2O$) and ammonium hydroxide (NH_4OH) as the starting materials were purchased from Merck Specialities Private Limited, Mumbai, India, starch soluble as capping agent and double-distilled water as dispersing solvent was used to prepare starch-capped Cu doped ZnO NP

purchased from Merck Specialities Private Limited, Mumbai, India.

Synthesis of starch-capped Cu doped ZnO

The synthesis of NP was carried out by a simple wet chemical method, 100 ml of 0.1 mol solution of $Zn(NO_3)_2 \cdot 6H_2O$ as a zinc source was stirred constantly for 30 min at 60 °C (solution **A**). 2 wt% of starch was stirred constantly at 60 °C for 2 hr (solution **B**). Now NH_4OH was slowly added drop by drop into the solution **A** and stirred at room temperature for 15 min and the pH of the solution was continuously measured. When the pH of the solution reached 7.5 and a white solution (solution **C**) was formed then pouring of NH_4OH was stopped. Then the mixture (solution **B** and solution **C**) was stirred constantly for 30 min at 60 °C (solution **D**) and separately for dopant 100 ml of 0.01 mol $CuCl_2 \cdot 2H_2O$ was stirred constantly for 30 minutes at 60 °C (solution **E**). The final mixture (solution **D** and solution **E**) was stirred constantly for 2 hr at 60 °C and allowed to cool down at room temperature till the light blue precipitate of Cu doped ZnO was formed. The whole solution was allowed to settle for overnight in a dark chamber. Finally, the precipitate was filtrated which was then washed with distilled water to dissolve the impurities and dried at 60 °C in oven for 12 hr.

Characterization

Powder X-ray diffraction (XRD) pattern of prepared ZnO nanoparticle has been recorded by Philips X-ray Diffractometer (X'Pert Pro) with Cu $K_{\alpha 1}$ radiation ($\lambda = 1.5406 \text{ \AA}$). Scanning electron microscope with EDAX (JSM -6360, Jeol) and Transmission Electron Microscope (JEM-2100, Jeol) have been used for the study of surface morphology, composition of elements and confirmation of NP respectively. The optical absorption spectrum of ZnO dispersed in water was recorded by a UV-vis spectrophotometer (HITACHI U - 3210). Room temperature PL spectroscopy was measured using Fluorescence Spectrophotometer (HITACHI F-2500) at an excitation wavelength of 300 nm.

Preparation of inoculums and culture media

The test organisms were grown in 5 ml Luria Bertani Broth at 37 °C and 0.5 McFarland' turbidity standard was used during antibacterial susceptibility test. Mueller Hinton Agar medium was the choice of media used in the antibacterial tests. All the culture media were purchased from HiMedia Pvt. Ltd., Mumbai, India.

Antibacterial activity assay

The anti-biogram experiment was done by well-diffusion method. Wells were made and filled with samples in a concentration of 40 mg/ml, 30 mg/ml and 20 mg/ml each. After 24 hr incubation the zone of inhibition (ZOI) was measured.

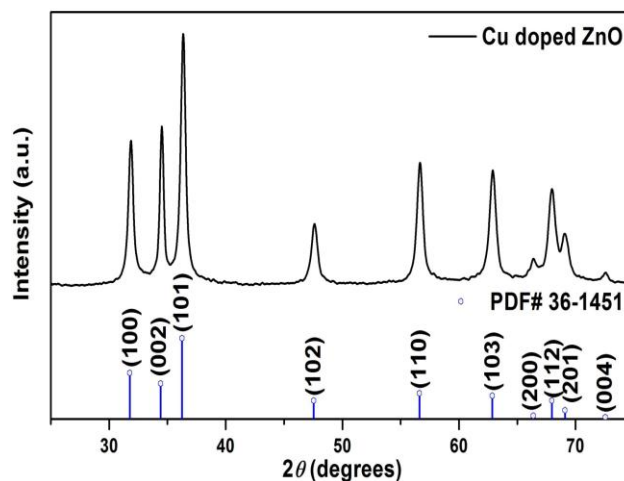


Fig. 1. XRD pattern of Cu doped ZnO NP.

Results and discussion

Structural, morphological and compositional studies

The XRD pattern of starch-capped Cu doped ZnO has been recorded in the range of 25°-75° (2θ) at a scanning rate of 0.02°/s and 0.5 sec/step as shown in Fig. 1. All the peaks corresponding to (100), (002), (101), (102), (110), (103), (200), (112), (201) and (004) planes are well indexed with the Powder Diffraction File (PDF No. 36-1451), indicating hexagonal wurtzite phase of ZnO with space group $P6_3mc$ (186) and no other diffraction peaks corresponding to Cu related secondary and impurity phases except ZnO has been detected, which revealed that the Cu^{2+} ions have substituted into the Zn lattice sites without affecting the crystal structure of ZnO. This may be due to the fact that ionic radius of Cu^{2+} (0.73 Å) is very close to that of Zn^{2+} (0.74 Å), so Cu can easily penetrate into the ZnO lattice [11]. The crystallite size of sample has been calculated by using the peak broadening of the peaks in the XRD pattern. This can be done according to the well established method of Scherrer [12]. The average crystallite size of the NP has been found to be ~ 15.51 nm from the (100), (002) and (101) indexed planes.

Fig. 2 (a) represents the surface of as-prepared sample which reveals that there is large homogeneity at the surface with a lot of particle agglomeration. The EDAX analysis depicted in Fig. 2 (b) shows presence of only Zn, Cu and O as expected for Cu doped ZnO NPs. No other impurity elements are present in the samples. It is observed that the as-prepared Cu doped ZnO NP is non-stoichiometric. The Cu/Zn weight percentage ratio has been found to be 9.64% in 10% molar Cu source doped in ZnO, which reveals the presence of Cu in the ZnO system and wt % is nearly equal to their nominal stoichiometry within the experimental error. Therefore, the EDAX spectrum shows well agreement with experimental concentration used for Cu doped ZnO system.

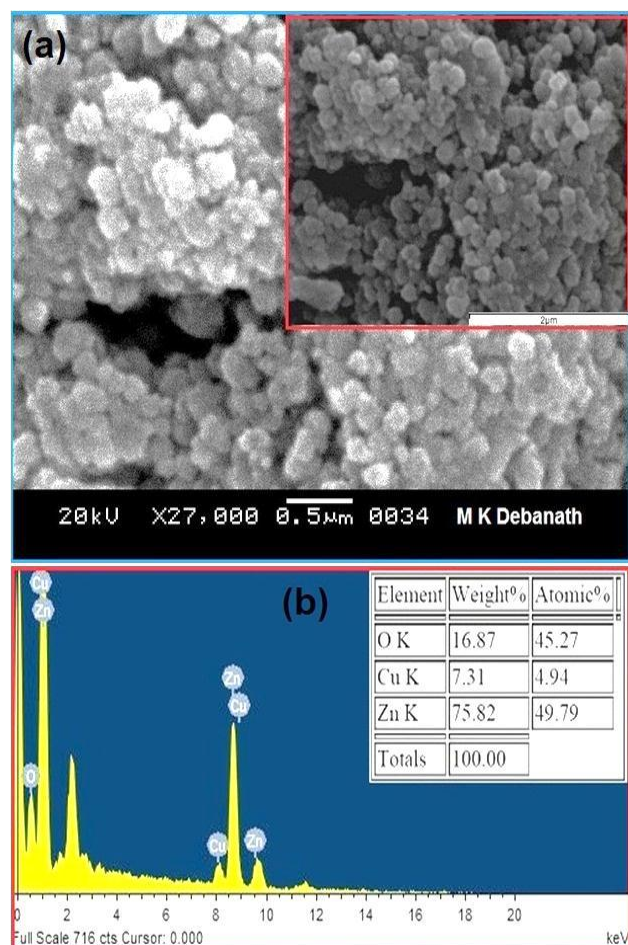


Fig. 2. (a) SEM image and (b) EDAX taken from inset of (a).

Fig. 3 shows HRTEM images of as-prepared sample ZnO:Cu. HRTEM images in Fig. 3 (a) & (b) show overlapping of smaller elongated hexagonal type Cu doped ZnO NPs that combined together to form a single hexagonal plate like Cu doped ZnO NP. The particle size calculated from HRTEM image for single hexagonal plate like structure has been found to be ~ 80.2 nm, whereas it is less than ~ 35.1 nm in breadth for individual elongated hexagonal Cu doped ZnO as shown in Fig. 3 (b). The SAED pattern shown in Fig. 3 (d) and HRTEM image of a single hexagonal plate like structure of Cu doped ZnO NPs shown in Fig. 3 (a) reveals that the NPs are crystalline in nature and are in wurtzite phase. The calculated d-spacing of the crystal plane from Fig. 3 (c) have been found to be ~ 0.24 nm, which represents the preferable crystal growth that closely matches with the plane (101) of ZnO.

Optical studies

The UV-vis absorption spectrum of as-prepared sample is shown in Fig. 4. It is seen that strong peak absorbance wavelength at ~ 294.5 nm, which indicates the presence of blueshift with decrease in particle sizes with respect to bulk ZnO (wavelength ~ 376 nm; 3.3 eV) and this could be attributed to the confinement effects [13, 14]. The

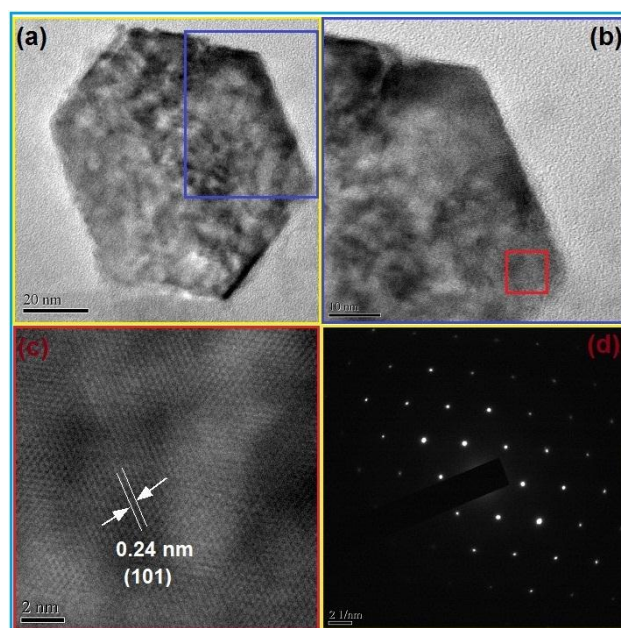


Fig. 3. (a) & (b) HRTEM images, (c) lattice and (d) SAED taken from inset of (a).

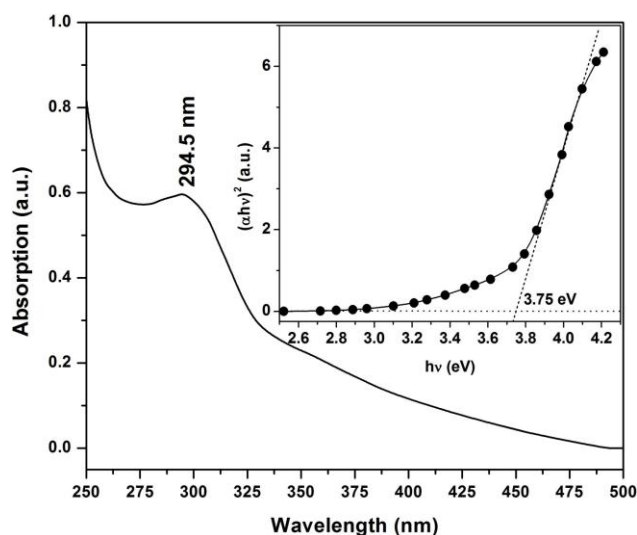


Fig. 4. UV-vis spectrum of Cu doped ZnO (Inset: plot to determine direct band gap).

direct band gap of sample is estimated from the graph (shown inset in Fig. 4) of $h\nu$ versus $(\alpha h\nu)^2$ for the absorption coefficient α which is related to the band gap E_g as $(\alpha h\nu)^2 = k(h\nu - E_g)$, where $h\nu$ is the incident light energy and k is a constant. The extrapolation of the straight line in Fig. 4 inset to $(\alpha h\nu)^2 = 0$ gives the value of band gap energy E_g . The optical band gap (E_g) have been found to be size dependent and there is an increase in the band gap (compared with bulk) of the semiconductor with a decrease in particle size. The optical band gap value obtained for starch-capped Cu doped ZnO is ~ 3.75 . Such an increase in the band gap energy is in good agreement with the corresponding blueshift seen in the absorption spectra mentioned above.

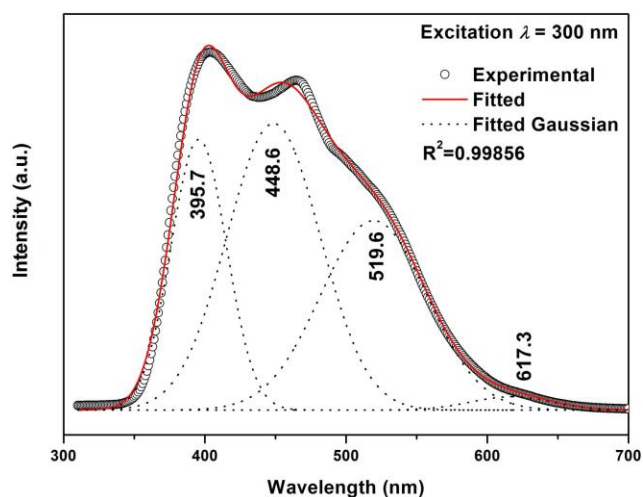


Fig. 5. Room temperature PL spectrum of Cu doped ZnO (The Gaussian peaks marked as dotted curves at the bottom of the fitted curve marked with red colour).

Fig. 5 shows the room temperature PL spectrum under excitation wavelength of 300 nm for ZnO:Cu sample which can be fitted by Gaussian peaks. The position of peaks centers are estimated to be at ~ 395.7 nm (3.13 eV), ~ 448.6 nm (2.76 eV), ~ 519.6 nm (2.39 eV) and ~ 617.3 nm (2.01 eV) respectively. The ultra violet emission peak at ~ 395.7 nm associated with near-band-edge (NBE) emission [11, 15], while blue emission peak at ~ 448.6 nm indicates the direct recombination of a conduction electron in the conduction band and a hole in the valance band or emission due to Zn interstitials [15, 16]. The green PL peak appearing at ~ 519.6 nm in the starch-capped sample is associated with oxygen vacancy (V_O) [15] and yellow emission peak at ~ 617.3 nm is due to oxygen interstitials (O_i) [17].

Antibacterial study

The ability of as-prepared sample as antibacterial agent to rupture bacterial cell have been tested by well-diffusion method in which ZnO:Cu sample with three different concentrations 40 mg/ml, 30 mg/ml and 20 mg/ml each were tested on Gram-positive bacteria *Staphylococcus aureus* (*S. aureus*) and Gram-negative bacteria *Escherichia coli* (*E. coli*). **Fig. 6** shows the well-diffusion tests of as-prepared NP at different concentrations dispersed in distilled water. The presence of ZOI clearly indicates the antibacterial effect of as-prepared sample. The results are summarized in **Table 1**. It has been observed that increasing the concentration of sample in wells, the ZOI has also been increased and was different according to the type of bacteria. In addition, increasing concentration of NP will result in large surface to volume ratio that can accumulate on the bacteria, killing it faster than lower concentrated NP. The antibacterial effect of ZnO:Cu NP arises due to the destruction effect of ZnO:Cu NP on the bacterial cells and increased production of active oxygen such as hydrogen peroxide (H_2O_2) which leads to the penetration of particles into the

cell membrane of bacteria. This leads to the formation of injuries resulting in the death of bacterium [18, 19].

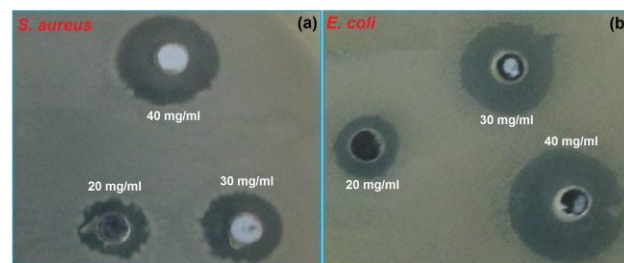


Fig. 6. Antibacterial activity of sample at different concentrations (40 mg/ml, 30 mg/ml and 20 mg/ml) against (a) *S. aureus* and (b) *E. coli*.

Table 1. Zone of inhibition (ZOI) for *S. aureus* and *E. coli*.

Bacteria	ZOI (mm) at concentration		
	40 mg/ml	30 mg/ml	20 mg/ml
<i>S. aureus</i>	18	15	12
<i>E. coli</i>	23	19	13

Conclusion

We have successfully synthesized starch-capped Cu doped ZnO NPs by simple wet chemical route for its structural, optical and antibacterial studies. The as-prepared sample was found to be in the hexagonal phase of ZnO with space group P63mc and no other Cu related impurities were detected from XRD and EDAX studies. The as-prepared NPs indicate the presence of blueshift with respect to bulk ZnO. It is also found to exhibit UV emission as well as defect related emissions from PL spectroscopy study. Therefore, the NPs can have wide applications in different optoelectronic devices. Results in our present study indicates that ZnO:Cu NPs show strong antibacterial activity against *S. aureus* and *E. coli* in which the activity increased as the concentration of ZnO:Cu NPs increased. In future, ZnO:Cu NPs might replace conventional antibiotics in humans and animals.

Acknowledgements

The authors thank the SAIF, Department of Instrumentation & USIC, Gauhati University; SAIF, NEHU Shillong; Department of Chemistry, Gauhati University for providing XRD, SEM with EDAX and TEM, UV- vis and PL spectroscopy measurements facilities respectively. The authors also thank the Department of Bioengineering and Technology, Gauhati University for providing laboratory facility and for the analyses of antibacterial activity.

Author's contributions

Conceived the plan: MKD, RKS, SMB, ES, KKS; Performed the experiments: MKD, KKS; Data analysis: MKD, ES, SMB, KKS; Wrote the paper: MKD. Authors have no competing financial interests.

Supporting information

Supporting informations are available from VBRI Press.

References

1. Khan, M. F.; Hameedullah, M.; Ansari, A. H.; Ahmad, E.; Lohani, M. B.; Khan, R. H.; Alam, M. M.; Khan, W.; Husain, F. M.; Ahmad, I.; *Int. J. Nanomed.* **2014**, *9*, 853.
DOI: [10.2147/IJN.S47351](https://doi.org/10.2147/IJN.S47351)
2. Kant, S.; Kumar, A.; *Adv. Mat. Lett.* **2012**, *3(4)*, 350.
DOI: [10.5185/amlett.2012.5344](https://doi.org/10.5185/amlett.2012.5344)
3. Park, Y. S.; Litton, C. W.; Collins, T. C.; Reynolds, D. C.; *Phys. Rev.* **1965**, *143*, 512.
DOI: [10.1103/PhysRev.143.512](https://doi.org/10.1103/PhysRev.143.512)
4. Shah, A. H.; Manikandan, E.; Ahmed, M. B.; Ganesan, V.; *J. Nanomed. Nanotechnol.* **2013**, *4(3)*, 1.
DOI: [10.4172/2157-7439.1000168](https://doi.org/10.4172/2157-7439.1000168)
5. Z. Emami-Karvani, P. Chehraz, *African J. Microbio. Res.* **2011**, *5(12)*, 1368.
DOI: [10.5897/AJMR10.159](https://doi.org/10.5897/AJMR10.159)
6. Yousef, J. M.; Danial, E. N.; *J. Health Sciences.* **2012**, *2(4)*, 38.
DOI: [10.5923/j.health.20120204.04](https://doi.org/10.5923/j.health.20120204.04)
7. Zhang, L.; Jiang, Y.; Ding, Y.; Povey, M.; York, D.; *J. Nanopart. Res.* **2007**, *9*, 479.
DOI: [10.1007/s11051-006-9150-1](https://doi.org/10.1007/s11051-006-9150-1)
8. Carvalho, P.; Sampaio, P.; Azevedo, S.; Vaz, C.; Espinós, J. P.; Teixeira, V.; Carneiro, J. O.; *Appl. Surface science* **2014**, *307*, 548.
DOI: [10.1016/j.apsusc.2014.04.072](https://doi.org/10.1016/j.apsusc.2014.04.072)
9. Raghupathi, K. R.; Koodali, R. T.; Manna, C.; *Langmuir* **2011**, *27*, 4020.
DOI: [10.1021/la104825u](https://doi.org/10.1021/la104825u)
10. Vidya, K.; Saravanan, M.; Bhoopathi, G.; Devarajan, V. P.; Subanya, S.; *Appl. Nanosci.*, **2015**, *5*, 235.
DOI: [10.1007/s13204-0014-0312-7](https://doi.org/10.1007/s13204-0014-0312-7)
11. Muthukumar, S.; Gopalakrishnan, R.; *Opt. Mat.* **2012**, *34*, 1946.
DOI: [10.1016/j.optmat.2012.06.004](https://doi.org/10.1016/j.optmat.2012.06.004)
12. Klug, H. P.; Alexander, L. E.; X-ray Diffraction Procedures for Polycrystalline and Amorphous Materials; Wiley: New York, 2nd ed., 1954.
13. Debanath, M. K.; Karmakar, S.; *Mater. Lett.* **2013**, *111*, 116.
DOI: [10.1016/j.matlet.2013.08.069](https://doi.org/10.1016/j.matlet.2013.08.069)
14. Gu, Y.; Kuskovsky, I. L.; Yin, M.; O'Brien, S.; Neumark, G. F.; *Appl. Phys. Lett.* **2004**, *85*, 3833.
DOI: [10.1063/1.1811797](https://doi.org/10.1063/1.1811797)
15. Kundu, S.; Sain, S.; Satpati, B.; Bhattacharyya, S. R.; Pradhan, S. K.; *RSC. Adv.* **2015**, *5*, 23101.
DOI: [10.1039/c5ra01152c](https://doi.org/10.1039/c5ra01152c)
16. Sabri, N. S.; Yahya, A. K.; Talari, M. K.; *J. Lumin.* **2012**, *132*, 1735.
DOI: [10.1016/j.jlumin.2012.02.020](https://doi.org/10.1016/j.jlumin.2012.02.020)
17. Ahn, C. H.; Kim, Y. Y.; Kim, D. C.; Mohanta, S. K.; Cho, H. K.; *J. Appl. Phys.* **2009**, *105*, 013502.
DOI: [10.1063/1.3054175](https://doi.org/10.1063/1.3054175)
18. Williams, D. N.; Ehrman, S. H.; Holoman, T. R. P.; *J. Nanobiotechnol.* **2006**, *4(3)*, 1477.
DOI: [10.1186/1477-3155-4-3](https://doi.org/10.1186/1477-3155-4-3)
19. Jin, J.; Liu, W.; Zhang, W.; Chen, Q.; Yuan, Y.; Yang, L.; Wang, Q.; *J. Nanopart. Res.* **2014**, *16*, 2658.
DOI: [10.1007/s11051-014-2658-x](https://doi.org/10.1007/s11051-014-2658-x)